USING SOLAR ENERGY FOR WATER PURIFICATION THROUGH NANOPARTICLES ASSISTED EVAPORATION: THEORETICAL AND EXPERIMENTAL INVESTIGATIONS

A THESIS SUBMITTED IN PARTIAL FULFILLMENT OF REQUIREMENTS FOR THE DEGREE OF

MASTER OF ENGINEERING

IN THERMAL ENGINEERING

BY

VIRENDER OHRI

REGISTRATION NO.: 801683029

UNDER THE SUPERVISION OF

DR. VIKRANT KHULLAR

(ASSISTANT PROFESSOR)

MECHANICAL ENGINEERING DEPARTMENT

THAPAR INSTITUTE OF ENGINEERING AND TECHNOLOGY, PATIALA-147004, PUNJAB, INDIA

CERTIFICATE

I hereby declare that the dissertation entitled "**Using Solar Energy For Water Purification Through Nanoparticles Assisted Evaporation:** Theoretical And Experimental Investigations" is an authentic record of my work carried out as requirements for the award of the degree of **Master of Engineering** in **Thermal Engineering** at **Thapar Institute of Engineering and Technology, Patiala** under the supervision of **Dr. Vikrant Khullar (Assistant Professor, Mechanical Engineering Department).** No part of the matter embodied in this report has been submitted to any other university or institute for the award of any degree.

Date: 15-JUNE-2018

Virender Ohri

Roll No.801683029

Thapar Institute of Engineering and Technology, Patiala

It is certified that the above statement made by the student is correct to the best of my knowledge and belief.

15/06/2018

Dr. Vikrant Khullar
Assistant Professor
Mechanical Engineering Department
Thapar Institute of Engineering and Technology, Patiala

ABSTRACT

As per the estimates of the world health organization (WHO); by 2025, about half of the world's population shall inhabit water stressed areas. Water purification through usage of solar energy is a clean and lucrative option to ensure access to clean and safe drinking water. In most of the solar energy driven desalination systems, evaporation of water is one of the key processes. In this direction, we propose that addition of nanoparticles into the water (owing to their enhanced thermo-physical properties and optical tune-ability) could significantly enhance the evaporation rate and thus the pure water yield. In the present work, we have developed a detailed theoretically model to predict (and quantify) the evaporation rates when water/nanoparticles dispersion directly interact with solar irradiance. In order to clearly gauge the effects of adding nanoparticles, two systems have been studied (i.e. the one with and the other without nanoparticles dispersed in water) under similar operating conditions. Theoretical calculations show that addition of even trace amounts of nanoparticles (volume fraction = 0.0001) into water can significantly enhance (57-58% higher than the pure water case) the evaporation rates and the pure water yield. Furthermore, a detailed parametric study involving host of parameters influencing the evaporation rate reveals that nanoparticle volume fraction and solar irradiance are the most impacting parameters. The results of the developed theoretical model have been compared with the experimental results in the literature, the two have been found to be in good agreement except at high nanoparticle volume fractions. For completeness, proof-of-the -concept experiments simulating the theoretical model have also been carried out. Finally, experiments under the sun have been carried out to clean sewage water through evaporation via volumetric absorption process. The pH and total dissolved solids (TDS) measurements of the distillate collected though the aforementioned process revealed that indeed impure water (such as sewage water in the present work) could be effectively cleaned through nanoparticles assisted evaporation.

ACKNOWLEDGEMENTS

I would like to express my special thanks and sense of gratitude to my supervisor, Dr. Vikrant Khullar for the guidance. I have been extremely lucky to have a supervisor who helped me in my work and I came to know about so many new things. He provided me the technical support, facilities and skills that really helped me during the work. He also provided the technical equipments that helped me to do experiments such as data acquisition system, analytical balance, optical fiber and lab to do the experiments. He cared so much about my work over the year. His patience, the adjustments he made, and trust and confidence he had in me really helped me to finish my work at the right time.

Furthermore I would like to express my sincere gratitude to the Mechanical Engineering Department, Thapar Institute of Engineering and Technology for the technical support. My special thanks to Dr. Madhup Kumar Mittal and Mr. Charanjeet Singh for providing hygrometer, which helped me to carry out relative humidity measurements. Also, my special thanks to Dr. V. K. Sanghal and Ms. Mitali Sarkar for helping me in doing pH and TDS measurements. Further, I would like to thank my lab. members Nirmal, Apoorava Amandeep, for their technical and moral support. Finally, I would like to express my sincerest sense of gratitude to my family for their support and love for me, without which this work could not have been possible.

TABLE OF CONTENTS

LIST OF FIGURES

LIST OF TABLES

NOMENCLATURE

English Symbols

A	Area of container [m^2]
c_p	Specific heat [$kJkg^{-1}K^{-1}$]
C_o	Cross section of particle [m^2]
D_{AB}	Mass diffusivity [m^2s^{-1}]
d	Diameter of particle [m]
dy	Node thickness along the depth direction [m]
dt	Time to evaporate dy thickness of water [s]
f_v	Volume fraction of nanoparticles in water
Gr	Grashof number
g	Acceleration due to gravity [ms^{-2}]
h_∞	Convective heat transfer coefficient [$Wm^{-2}K^{-1}$]
h_{fg}	Latent heat of vaporization [$kJkg^{-1}$]
h_{mass}	Mass transfer coefficient [$m\ s^{-1}$]
I_λ	Intensity of solar radiation [Wm^{-2}]
k	Thermal conductivity [$Wm^{-1}K^{-1}$]
K_λ	Spectral optical coefficient [m^{-1}]
L_c	Characteristic length [m]
m	Normalized refractive index of fluid
mv	Evaporation rate [kgs^{-1}]
Nu	Nusselt number
N_o	Number density of particle
n	Index of refraction
P	Pressure [Nm^{-2}]
Pr	Prandtl number
Q	Efficiency
Re	Reynolds number
Sc	Schmidt number
Sh	Sherwood number
s	Path length [m]
T	Temperature [°C]

Greek Letters

α	Size parameter
λ	Wavelength of solar radiation [μm]
v	Momentum diffusivity [m^2s^{-1}]
κ	Index of absorption
ρ	Density [kgm^{-3}]

Subscripts

abs	Absorption
co	Combined free and forced convection
e	Extinction
fo	Forced convection
fr	Free convection
nd	Nanoparticle dispersion
np	Nanoparticle
s	Surface
sat	Saturation
sca	Scattering
v	Vapour
w	Water

Abbreviations

NIR	Near infrared
PTM	Present theoretical model
RH	Relative humidity
RTE	Radiative transfer equation
UV	Ultra violet
VIS	Visible

CHAPTER 1
INTRODUCTION

1.1. MOTIVATION

1.1.1 WATER SCARCITY

Water scarcity is the non availability of fresh water to satisfy the basic needs of people in a particular region. Continuously rising demand and increasing agriculture land are the main reasons for water scarcity. Shortage of water can be either due to insufficient natural water resources in a particular region or due to improper utilization of available water resources. Actually, improper utilization of water is found to be the main reason of shortage of water. Today, many regions of India are facing water scarcity that is seriously worse than the past decades. Ground water situation is even worse than surface water. Water resources are continuously reducing. Whereas industries make water more polluted. Ground water is being continuously contaminated by industrial pollutants, which is increasing the potential health risks to humans and bio-diversities. It is therefore, imperative to conserve and replenish portable water.

1.1.2 WATER PURIFICATION

Now a day's water purification is necessary to use it for a particular application, either it is used for drinking and other household purposes or it is used for industrial/agricultural purposes. For each purpose water must be purified up to certain level. For drinking, water must be pure and should have some minerals that are essential for body. Whereas for agriculture water should be fit for crops and should not have harmful chemicals. Thus in the process of water purification dirty water is processed to use it for specific purposes. In waste water, biological contaminants, suspended solids, undesirable chemicals and gases may be present and is therefore not fit for drinking and other purposes. Water purification systems must be devised according to the requirements of the application in hand; chemical and industrial applications, medical and pharmacological applications etc, all have different requirements. There are many methods that can be used to purify the water such as sedimentation, distillation, slow sand filters, chemical processes such as flocculation and chlorination, the use of ultra violet light and filtration etc.

During purification there must be reduction in the concentration of dissolved solid particles, biological cells such that viruses, fungi and bacteria etc. At present, for every purpose (for household/industrial/agricultural use), water quality is measured according to the standards set by the governments. It cannot be decided visually that whether water is safe for a particular need. Thus it is necessary to test the water chemically and biologically before it is to be used for a particular application. Visual inspection cannot determine if water is of appropriate quality. Although numerous water purification techniques available, most of them are either limited to purifying waste water from a particular application (such as tap water, discharge from a particular industry, saline water, waste water etc.) and also are energy intensive and costly [1-6]. Therefore, more cost effective and lesser energy intensive technology that can handle range and levels of impurities is required. Evaporation and subsequent condensation is one such method

which can prove to be cost effective, at the same time utilize renewable energy (such as solar energy), and handle range of impurities. In the present work, the role of nanoparticles in enhancing the evaporation rate of water has been theoretically and experimentally analyzed. It has been found that the present method is effective in purifying sewage water, which represents a mixture of a host of impurities, chemicals etc through direct interaction with the solar irradiance.

1.2 THESIS OUTLINE

Chapter 1 gives the motivation behind the present thesis work. It includes reasons, process and need of the present work that is water purification by evaporating the water. Chapter 2 is the review of the literature which I have gone through during my thesis work. This process has given me diverse perspectives, data and much useful information related to my present work. Theoretical model formulation has been presented in Chapter 3. This chapter gives the methodology, formulation and assumptions that were used to model the evaporation process. It describes the theoretical steps by which evaporation rate of water or nanofluid can be formulated. Formulation is done for evaporation process using Fick's law. On the other hand to volumetrically heat the amorphous carbon nanofluid or pure water, Lambert Beer law and overall energy balance equations have been invoked. Chapter 4 describes the numerical modeling and discretisation techniques involved. It includes the algorithm that was implemented by writing a code in MATLAB. Chapter 5 gives the results and outcomes of the theoretical modeling. It shows the evaporation rates and temperature distributions under different operating conditions. It reveals the whole evaporation process and details the time to evaporate fixed amount of water at different temperatures. It shows the results at different conditions such as different volume fractions, air velocity, relative humidity and solar intensities. Chapter 6 is about experimental work. It describes in detail the equipments used, methods, materials used. Chapter 7 reveals the experimental results and outcomes. It shows the graphs of evaporation rate and temperature distributions. Chapter 8 details the validation of the developed theoretical model, proof-of-the-concept indoor and outdoor experiments. Chapter 9 details the conclusion of the present work.

CHAPTER 2
LITERATURE REVIEW

2.1 INTRODUCTION

Although intermittent, solar energy is a clean and abundant renewable energy resource. In the backdrop of the improvements in the solar thermal energy harnessing technologies, it is envisaged that in years to come, it shall play a significant (and more tangible) role in host of applications ranging from cooking, water heating, air-conditioning, electricity generation and water desalination. Among these, water purification is one of the most critical applications wherein solar energy could be put to use to improve the quality of drinking water especially in rural and water stressed regions of the globe where the deployment of state of the art water purification systems is not a viable and cost effective proposition. Conventional solar desalination systems have relatively low pure water yields. Over the years, these systems have undergone various design modifications with the objective of further improving the pure water yield [1-21]. In conventional solar stills, solar energy heats the water indirectly (an intervening solar selective surface first absorbs the solar energy and then transfer to the water through conduction), resulting in evaporation (and hence purification) of the water, subsequently this water in vapor form is collected with the help of condensation on to an inclined cooled surface. Table 1 List down notable researchers along with their affiliation who are active in studying solar driven desalination systems.

Table 1: List of the notable researchers (along with their affiliations) who are actively working for purification of water by solar desalination processes

S. No.	Title of the research paper	Institute/University/Laboratory	Researcher(s)
1.	An Experimental Study of a Solar Still: Application on the sea water desalination of Fouka.	Solar Equipement Develpement Unit, UDES, National road Tipaza, Algéria.	Aburideh,H., Deliou, A.,Abbad,B., Alaoui, F., Tassalit , D. and Tigrine, Z.
2.	Distillate water quality of a single- basin solar still: laboratory and field work.	New Maxico State University Las Cruces USA	Hanson, A., Zachritz, W., Stevens, K., Mimbela, L., Polka, R., Cisneros, L.
3.	Enhancement of distillate output of double basin solar still with vacuum tubes.	Gujarat Power Eng. And Research Institute, Mehsana, Gujarat, India.	Panchal, H., N.
4.	Enhancing the design to optimize the performance of double basin solar still.	Sathyabama University, Chennai, India.	Joe Patrick Gnanaraj, S.,Ramachandran, S., Santosh Christopher, D.
5.	Experimental performance and investigation of tilted solar still with basin and wick for distillate quality and enviro-economic aspects.	Indian Institute of Technology Madras Chennai India.	Sharon, H., Reddy, K., S., Krithika,D., Philip,L.

2.2 APPLICABILITY OF NANOPARTICLES

Owing to the tunable optical properties and very high convective heat transfer coefficients, the nanoparticles can effectively absorb and readily transfer that absorbed solar energy [22-26] to the water and hence considerably enhance the evaporation rates and the pure water yield. In other words, direct volumetric absorption by the nanoparticle dispersion could actually enhance the evaporation rates. Recently, few researchers have shown that addition of nanoparticles to the basefluid could actually enhance the evaporation rates [27, 28] (see Table 2) but there is no theoretical model which could quantify (and hence predict) evaporation rates during volumetric heating (particularly in case of nanofluids).

Table 2 List the notable researchers along with their affiliation who are actively working in enhancing the evaporation by using nanoparticles.

S. No.	Title of research paper	Institute/University/ Laboratory	Researcher(s)
1.	Optical properties and radiation-enhanced evaporation of nanofluid fuels containing carbon-based nanostructures.	School of Aeronautics and Astronautics, Purdue University, West Lafayette, United States.	Gan,Y., and Qiao, Li
2.	Hydrophobically modified nanoparticle suspensions to enhance water evaporation rate.	University of Science and Technology,Beijing, China.	Huang, Z., Li, X., Yuan, H., Feng, Y.,and Xinxin
3.	Nanoparticlemediated evaporation at liquid–vapor Interfaces.	State University of New York at Binghamton, Binghamton, NY , United States.	Yong, X., Qin, X., T T.,J., Singler
4.	Modeling Evaporation and Particle Assembly in Colloidal Droplets.	Department of Mechanical Engineering, Binghamton University, Binghamton, New York United States	Zhao, M., and Yong X.
5.	Solar water heating and vaporization with silicon nanoparticles at mie resonances.	National Institute for Materials Science (NIMS), Tsukuba, Ibaraki , Japan	Ishii, S., Sugavaneshwar, R. P., Chen, K., Dao, T., D., Nagao, T.

2.3 THESIS OBJECTIVES

The present work explores the idea of enhancing the evaporation rate of water through addition of nanoparticles. Following are the specific objectives of the thesis:

- To develop a comprehensive theoretical model to quantify evaporation rate during volumetric absorption and also to find temperature distribution within the fluid.
- To identify key parameters that impacts the evaporation rate.
- To validate the theoretical modeling results with those available in the literature.
- Validation of the theoretical model by carrying out proof-of-the-concept experiments
- To carry out pH and total dissolved solids (TDS) measurements of the sewage water before and after the purification process.

CHAPTER 3
THEORETICAL MODELING

3.1 INTRODUCTION

In the present work we have developed a comprehensive theoretical model to quantify the evaporation process of water. Particularly, we report the impact of dispersing carbon-based nanostructures (amorphous carbon nanoparticles) on evaporation of water. Amorphous carbon nanoparticles have been chosen owing to their high absorptivity in the solar irradiance wavelength band [26]. We have investigated the evaporation rates of water at different volume fractions of these nanoparticles and under different ambient conditions. To quantitatively determine the wavelength-dependent absorption and scattering characteristics, we have used the optical constants (namely spectral index of refraction and index of absorption) of the nanoparticles and water [29-32]. Theoretical calculations reveal that there is significant enhancement in the evaporation rate of water when even trace amounts of nanoparticles are added. Furthermore, the comparison of the developed theoretical model with the experimental study available in the literature reveals that the results obtained from developed theoretical model quite closely approximates those available in the literature.

3.2 BASIC IDEA AND UNDERLYING ASSUMPTIONS

Figure 1(a) shows the schematic diagram of the evaporation process when solar irradiance directly (volumetrically) interacts with the nanoparticle dispersion. In the present work, it is assumed that the fluid (water or water + nanoparticles) is placed in a container of 1 cm depth and 1 m^2 aperture area. The side and bottom walls of the container are assumed to be insulated. The bottom surface has been made to be reflective, i.e., at the bottom surface, there is 3M solar mirror film which due to its good spectral reflectance in the solar irradiance wavelength band [see Fig. 1(b)] helps in increasing the optical depth, and hence increasing the magnitude of the solar irradiance absorbed by the fluid. Furthermore, solar irradiance directly interacts with the nanoparticle dispersion, i.e. solar irradiance either gets absorbed or scattered as it transverses through the liquid column (this absorbed energy represents the energy generation term in the overall energy balance equation). To quantify the terms of energy generation, simplified form of radiative transfer equation (RTE) i.e., Lambert Beer law has been employed. Scattering phenomenon has been approximated by Rayleigh scattering regime as the particle size is small compared to the incident wavelength [29-32].

3.3 MODELING FRAMEWORK

Evaporation process during volumetric heating is a highly coupled phenomenon. For given ambient conditions, the evaporation rate depends on the top layer of nanofluid. Top layer temperature in turn depends on the manner in which the solar irradiance gets absorbed in the nanoparticle dispersion. As the water gets evaporated, the concentration of the nanoparticles in the dispersion also changes and in turn effects the spatial distribution of the energy absorbed. Furthermore, the spatial temperature distribution is also influenced by the conduction of heat

within the nanoparticle dispersion as well as the convective losses to the surroundings and temperature drop due to phase change (i.e. evaporative cooling).

The theoretical modeling of the evaporation process essentially involves the following steps:

- calculation of convective mass and heat transfer coefficients
- quantification of the spatial energy generation term i.e. calculating the energy absorbed due to interaction of the solar irradiance with the nanoparticle dispersion
- solving the overall energy balance equation to find out the spatial temperature distribution

The subsequent sections essentially detail each of the aforementioned steps.

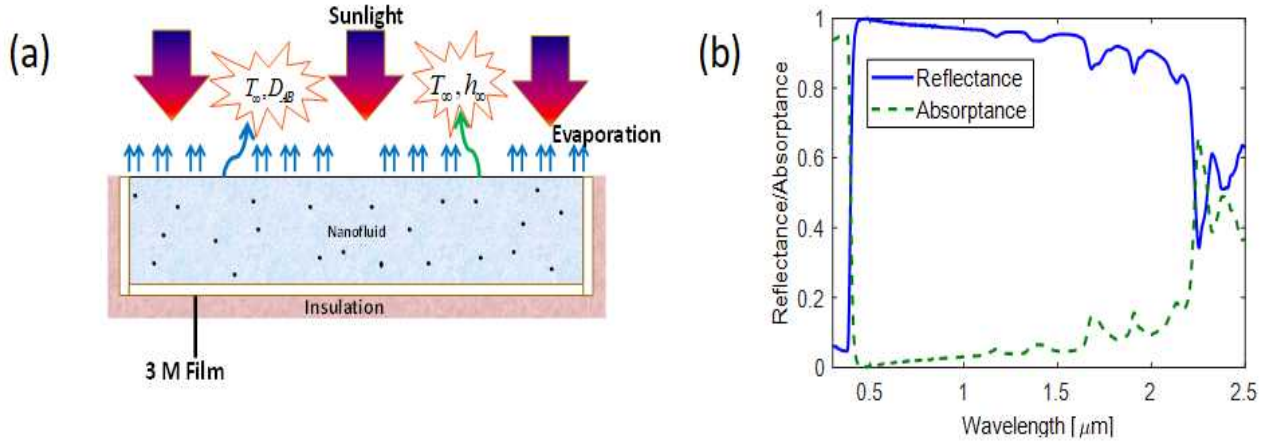

Fig. 1(a) Schematic showing the evaporation process when solar irradiance directly interacts with the nanoparticle dispersion, and (b) spectral reflectance (and absorptance) of 3M solar mirror film measured with UV-VIS-NIR spectrophotometer (PerkinElmer Lambda 1050).

3.4 MODELING MASS CONVECTION AND HEAT TRANSFER:

To quantify the evaporation rate, we have used the Fick's law of diffusion [33-34]. Evaporation rate depends on relative humidity and ambient air temperature. Also, evaporation rate increases with the increase in temperature of water. According to Fick's law of mass diffusion, the evaporation rate of water $(\dot{mv})$ changes with local mass concentration gradient $(\rho_{v,s} - \rho_{v,\infty})$ and is given by the following expression

$$\dot{mv} = h_{mass} A_s (\rho_{v,s} - \rho_{v,\infty}), \quad (1)$$

where h_{mass} represents the convective mass transfer coefficient, A_s represents surface area, densities at the surface and away from the surface of water could be calculated using Eqs. (2) – (4) and Eqs. (5) – (7) respectively.

$$\rho_{v,s} = \frac{P_{v,s}}{R_v T_s}, \tag{2}$$

$$\rho_{a,s} = \frac{P_{a,s}}{R_a T_s}, \tag{3}$$

$$\rho_s = \rho_{v,s} + \rho_{a,s}, \tag{4}$$

$$\rho_{v,\infty} = \frac{P_{v,\infty}}{R_v T_\infty}, \tag{5}$$

$$\rho_{a,s} = \frac{P_{a,\infty}}{R_a T_\infty}, \tag{6}$$

$$\rho_\infty = \rho_{v,\infty} + \rho_{a,s} \tag{7}$$

where the vapor pressure could be found through the following expression

$$P_v = P_{\text{sat}} \varphi \tag{8}$$

where P_{sat} represents pressure of water vapor at saturation for specified temperature.
Water vapors moves from a zone of higher vapor pressure towards a zone of lower vapor pressure. Schmidt number [expressed mathematically by Eq. (9)] is the ratio of molecular momentum and mass diffusion for particular boundary layer. If Schmidt number is one it means that mass transfer by diffusion is equal to the momentum transfer by diffusion.

$$Sc = \frac{\upsilon}{D_{AB}} = \frac{momentum\ diffusivity}{mass\ diffusivity}, \tag{9}$$

where D_{AB} is mass diffusivity and v is momentum diffusivity of air.

$$D_{AB} = 1.87 \times 10^{-10} \left[\frac{T^{2.072}}{P} \right]$$
$$for\ 280K \ \le \ T \ \le \ 450K \tag{10}$$

The diffusion coefficients are usually determined experimentally. Given the typical temperatures involved, the abovementioned empirical relation has been employed for the calculating the diffusion coefficient $D_{\text{H2O-air}}$ [34] in the present work.

Dimensionless number 'Sherwood number' quantifies the evaporation rate and is mathematically expressed by Eq. (11) as

$$Sh_{fr,fo,co} \ = \ \frac{h_{\text{mass}} L_c}{D_{AB}} \ , \tag{11}$$

where

$$L_c = \frac{A_s}{P} \tag{12}$$

is the characteristic length, D_{AB} represents the mass diffusivity and h_{mass} represents the mass transfer coefficient. The subscripts *fr*, *fo* and *co* denotes free, forced, and combined free and forced convection respectively.

Now for a given characteristic length and diffusion coefficient, evaluation of mass transfer coefficient necessitates Sherwood number to be known. Furthermore, Sherwood number is characteristic of the operational convection regime i.e. whether free, forced or combined free and forced convection. Sherwood number in case of the aforementioned convection regimes could be calculated using Eqs. (13), (14) and (15) respectively [33-38]

$$Sh_{fr} = 0.15\left(GrSc\right)^{1/3} \text{ for } \quad 10^7 < GrSc < 10^{11} \ , \tag{13a}$$

$$Sh_{fr} = 0.54(GrSc)^{1/4} \text{ for } \quad 10^4 < GrSc < 10^7 , \tag{13b}$$

$$Sh_{fo} = 0.664\,\mathrm{Re}^{1/2}\, Sc^{1/3} \text{ for } \quad \mathrm{Re} < 3\times10^5 , \tag{14a}$$

$$Sh_{fo} = 0.0296\,\mathrm{Re}^{4/5}\, Sc^{1/3} \text{ for } \quad \mathrm{Re} > 3\times10^5 \tag{14b}$$

$$Sh_{co} = (Sh_{fo}^4 + Sh_{fr}^4)^{1/4} \tag{15}$$

where Grashof and Reynolds numbers are is defined by Eqs. (16) and (17) respectively.

$$Gr = \frac{gL_c^3\left(\rho_\infty - \rho_s\right)}{\rho\upsilon^2} , \tag{16}$$

$$\mathrm{Re} = \frac{\rho u L_c}{\nu} , \tag{17}$$

During evaporation, heat is also convected to the ambient air. To quantitatively determine the heat transfer rate due to convection and coefficient of that heat transfer needs calculation. This could be done if Nusselt number [given by Eq. (18)] is known.

$$Nu_{fr,fo,co} = \frac{h_\infty L_c}{k} , \tag{18}$$

Nusselt number could be found using the following empirical relation

$$Nu_{fr} = 0.15\left(GrPr\right)^{1/3} , \tag{19}$$

$$Nu_{fo} = 0.332\sqrt{\mathrm{Re}}\,\mathrm{Pr}^{1/3} \text{ for } \quad \mathrm{Re} < 3\times10^5 , \tag{20a}$$

$$Nu_{fo} = 0.0296\,\mathrm{Re}^{4/5}\,\mathrm{Pr}^{1/3} \text{ for } \quad \mathrm{Re} > 3\times10^5 , \tag{20b}$$

$$Nu_{co} = (Nu_{fo}^4 + Nu_{fr}^4)^{1/4} , \quad (21)$$

where *Pr Re*, and *Gr* are the Prandtl, Reynolds and Grashof numbers respectively.

Finally, the evaporation rate and convective heat loss could found though Eqs. (22) and (23) respectively.

$$m\dot{v} = h_{mass} A_s (\rho_{v,s} - \rho_{v,\infty}) , \quad (22)$$

$$\dot{Q}_{con} = h_\infty A_s (T_s - T_\infty) \quad (23)$$

3.4 MODELING INTERACTION BETWEEN SOLAR IRRADIANCE AND THE NANOPARTICLE DISPERSION:

When solar irradiance interacts with a participating media such as water/nanoparticle dispersion, the solar radiant energy gets converted into the thermal energy in the fluid via absorption and scattering mechanisms. Amorphous carbon nanoparticles owing to their broad spectra absorption characteristics and high solar weighted absorptivity have been chosen in the present work. Furthermore, as low volume fractions of nanoparticles are involved in the theoretical work and nanoparticles size being small in comparison to the wavelength of the incident radiant energy, scattering could be approximated as independent scattering following Rayleigh scattering regime. The absorption of the solar irradiance as it transverses across the nanoparticle dispersion could be quantified through simplified form of radiative transfer equation (RTE) i.e. the Lambert beer law [22] given by Eq. (24) as

$$\frac{dI_\lambda}{ds} = -K_{e\lambda,nd} I_\lambda \quad (24)$$

where $K_{e\lambda,nd}$ is the spectral extinction coefficient of the nanoparticle dispersion, s is the path length and I_λ is the spectral intensity of the incident solar irradiance.

Extinction of the solar irradiance takes place due to absorption and scattering due to nanoparticles and absorption by the fluid. Mathematically, spectral extinction coefficient of the nanoparticle dispersion could be expressed as

$$K_{e\lambda,nd} = K_{abs\lambda,nd} + K_{sca\lambda,np} \tag{25}$$

where $K_{abs\lambda,nd}$, $K_{sca\lambda,np}$ are the spectral absorption and scattering coefficients of the nanoparticle dispersion and nanoparticles respectively. If absorbing nanoparticles are suspended in an absorbing continuous medium, then the absorption coefficient of the resulting nanoparticle dispersion could be approximated as volume-weighted average of the particles and continuous medium [29], mathematically given by Eq. (26) as

$$K_{abs\lambda,nd} = C_o N_o + \frac{4\pi\kappa_{\lambda w}}{\lambda}(1 - f_v) \tag{26}$$

where C_o, N_o, f_v denote the cross section, number density, and volume fraction of the nanoparticles respectively; and $\kappa_{\lambda w}$ is the spectral index of absorption of water. The absorption and scattering characteristics of the nanoparticles are often expressed as efficiency factors. The absorption (and scattering) efficiencies Q_{abs} (Q_{sca}) are defined as the ratio of the absorption cross section (scattering cross section) to the geometric projected area of the nanoparticle. Extinction efficiency, Q_e (=Q_{abs} + Q_{sca}) denoting the combined effect of absorption and scattering phenomena could be expressed as

$$C_o N_o = \frac{1.5 Q_e f_v}{d}, \tag{27}$$

where d denotes the hydrodynamic diameter of the nanoparticle (80nm in the present work). Furthermore, the extinction efficiency in the Rayleigh scattering regime is give by Eq. (23) as

$$Q_e = 4\alpha im\left[\frac{m^2-1}{m^2+2}\left\{1+\left(\frac{\alpha^2}{15}\right)\left(\frac{m^2-1}{m^2+2}\right)\left(\frac{m^4+27m^2+38}{2m^2+3}\right)\right\}\right], \tag{28}$$
$$+real\left[\frac{8}{3}\alpha^4\left\{\frac{m^2-1}{m^2+2}\right\}^2\right]$$

where m is the normalized spectral complex refractive of the nanoparticle and α is the size parameter.

Figure 2 details the calculated spectral extinction coefficients of nanoparticle dispersions at various nanoparticle volume fractions and that of pure water.

Now, once we have calculated the spectral extinction coefficients of nanoparticle dispersion, next we could use these to quantify the intensity attenuation as the solar irradiances transverses through the nanoparticle dispersion. The totality (across the entire solar irradiance wavelength band) of attenuation represents the energy generation term in the overall energy balance equation.

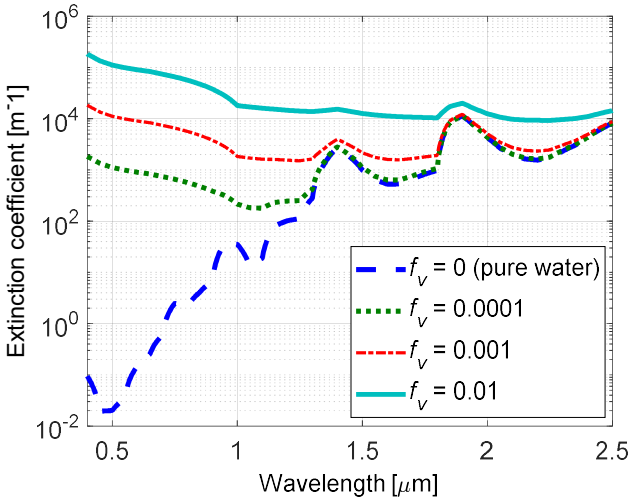

Fig. 2 Extinction coefficient as a function of wavelength for nanoparticle dispersions (amorphous carbon nanoparticles dispersed in water) at various volume fractions. The values of indices of absorption and indices of refraction for calculation of spectral extinction coefficients have been taken from Ref. [29-31]

CHAPTER 4
NUMERICAL MODELING

4.1 MODELING OVERALL ENERGY BALANCE TO FIND SPATIAL TEMPERATURE

An algorithm (see Fig. 3) has been devised which uses all the couplings among various heat and mass transfer processes that dictate the evaporation rates in MATLAB. A code was formulated in the MATLAB to apply this algorithm and find the temperature distribution with in the nanofluid and hence the evaporation rate as a function of time.

Firstly, the nanoparticle dispersion has been spatially discritized along the depth direction into finite number of nodes as shown in Fig. 4. Equations (29) and (30) represent the implicit finite difference form of the overall energy balance equations for the boundary (which is moving) and interior nodes respectively. In these equations *i* is for particular spatial node and *n* is for a particular time instant.

$$Ak_{nd}\frac{(T_i^{n+1}-T_{i-1}^{n+1})}{dy}+q_{gen,i-1}=h_\infty A(T_{i-1}^{n+1}-T_\infty)+h_{fg,nd}^{n}dyA\ , \tag{29}$$

$$\rho_{nd}dyAc_{p,nd}\frac{(T_i^{n+1}-T_i^{n})}{dt}=-Ak_{nd}\frac{(T_i^{n+1}-T_{i-1}^{n+1})}{dy}$$
$$+Ak_{nd}\frac{(T_{i+1}^{n+1}-T_i^{n+1})}{dy}+q_{gen,i} \tag{30}$$

where *dt* can be calculated using Eq. (26) as

$$dt=\frac{dyA}{m\dot{v}^n} \tag{31}$$

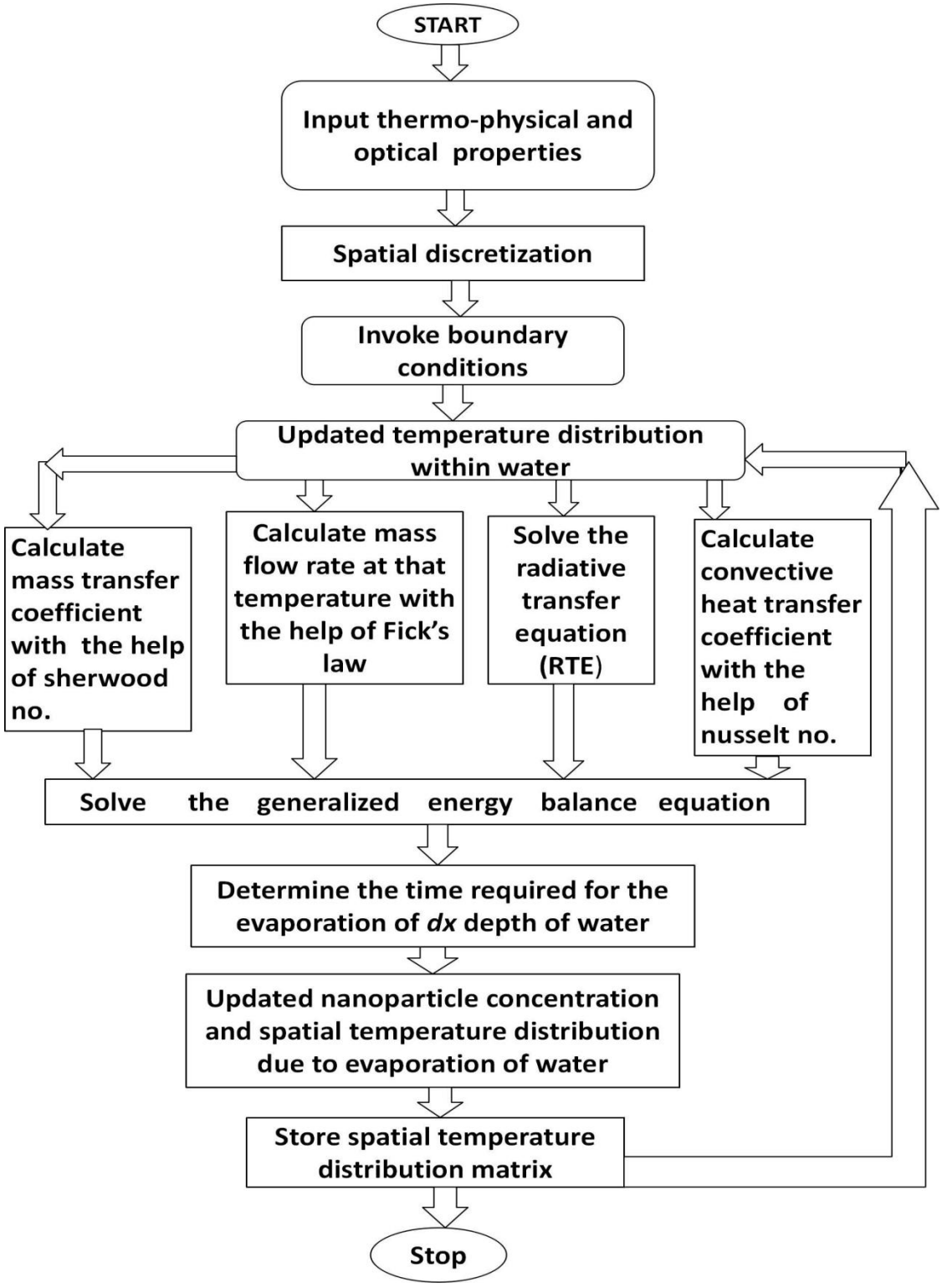

Fig. 3 Algorithm implemented in MATLAB for finding the evaporation rate and the spatial temperature distribution.

In the aforementioned equations, q_{gen} represents the energy generation term; k_{nd}, ρ_{nd}, $c_{p,nd}$ and $h_{fg,nd}$ denote the effective thermal conductivity, density, specific heat and latent heat of vaporization respectively of nanoparticle dispersion [38]. Mathematically, these could be expressed by Eqs. (32) - (35) as

$$\frac{k_{nd}}{k_w} = \frac{k_{np}\left(1+f_v\right)+2k_w\left(1-f_v\right)}{k_{np}\left(1-f_v\right)+k_w\left(2+f_v\right)}, \tag{32}$$

$$\rho_{nd} = \rho_w(1-f_v)+\rho_{np}f_v, \tag{33}$$

$$c_{p,nd} = \frac{\rho c_{p,w}(1-f_v)+\rho_{np}c_{p,np}f_v}{\rho_w(1-f_v)+\rho_{np}f_v}, \tag{34}$$

$$h_{fg,nd} = \frac{\rho_w h_{fg,w}\left(1-f_v\right)}{\rho_w\left(1-f_v\right)+\rho_{np}f_v} \tag{35}$$

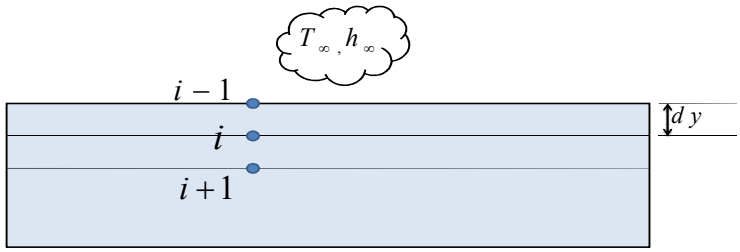

Fig. 4 Schematic showing the spatial discretization of nanoparticle dispersion.

CHAPTER 5
THEORETICAL RESULTS

5.1 INTRODUCTION

The heat and mass transfer mechanisms relevant to the evaporation process during volumetric heating have been modeled mathematically. Thus effect of adding nanoparticles on the evaporation rate of water have been computed (and quantified). For this, two cases (i.e. pure water and amorphous carbon based nanoparticle dispersion) have been compared under identical operating conditions (as detailed in Table 3). Time required to evaporate a fixed amount of water (~ 29 ml in the present study) has been calculated for the two cases. Furthermore, the evolution of spatial temperature distribution as evaporation takes place has also been computed to understand the heat transfer mechanisms involved.

Table 3. Geometrical details of the container housing the fluid (water/nanoparticle dispersion) and the operating conditions.

Aperture area	$1m^2$
Depth of fluid column	$1000\mu m$
Bottom and side walls	Insulated
Top surface	Exposed to the ambient
Bottom surface	Reflective, 3M solar mirror film
Volume of the water to be evaporated	~ 30ml
Ambient air relative humidity	55%
Ambient air temperature	27°C
Solar Irradiance, DNI	800 Wm^{-2}

Figure 5(a) shows the mass evaporated as a function of time in the two cases. It is clearly apparent from the curves that addition of nanoparticles considerable increases the evaporation rate. For ~ 30ml (30mg) of water to be evaporated, addition of even trace amounts (f_v = 0.0001) of amorphous carbon nanoparticles reduces the evaporation time by 57.7%. Furthermore, Figs. 5(b) and 5(c) detail the evolution of temperature profiles and depth of the liquid column in the two cases as the water gets evaporated. These curves reveal a very unique feature that differentiates the two cases. In the case of nanoparticle dispersion the highest temperature occurs at the free surface (and there is pronounced temperature gradient across the depth) whereas in the

case of pure water, the highest temperatures occur at the bottom (and there is very less temperature gradient across the depth). This may be attributed to the fact that in the former case the maximum absorption of the solar irradiance occurs in top layer, although some temperature drop does happen due to evaporative cooling, but the energy gain is far greater resulting in highest temperatures at the top. In the case of pure water, the medium itself is not a very good absorber of solar energy. Although here also the maximum energy absorption takes place in the top layer, but due to evaporative cooling from the top layer, the highest temperatures do not occur at the top but at the bottom layers.

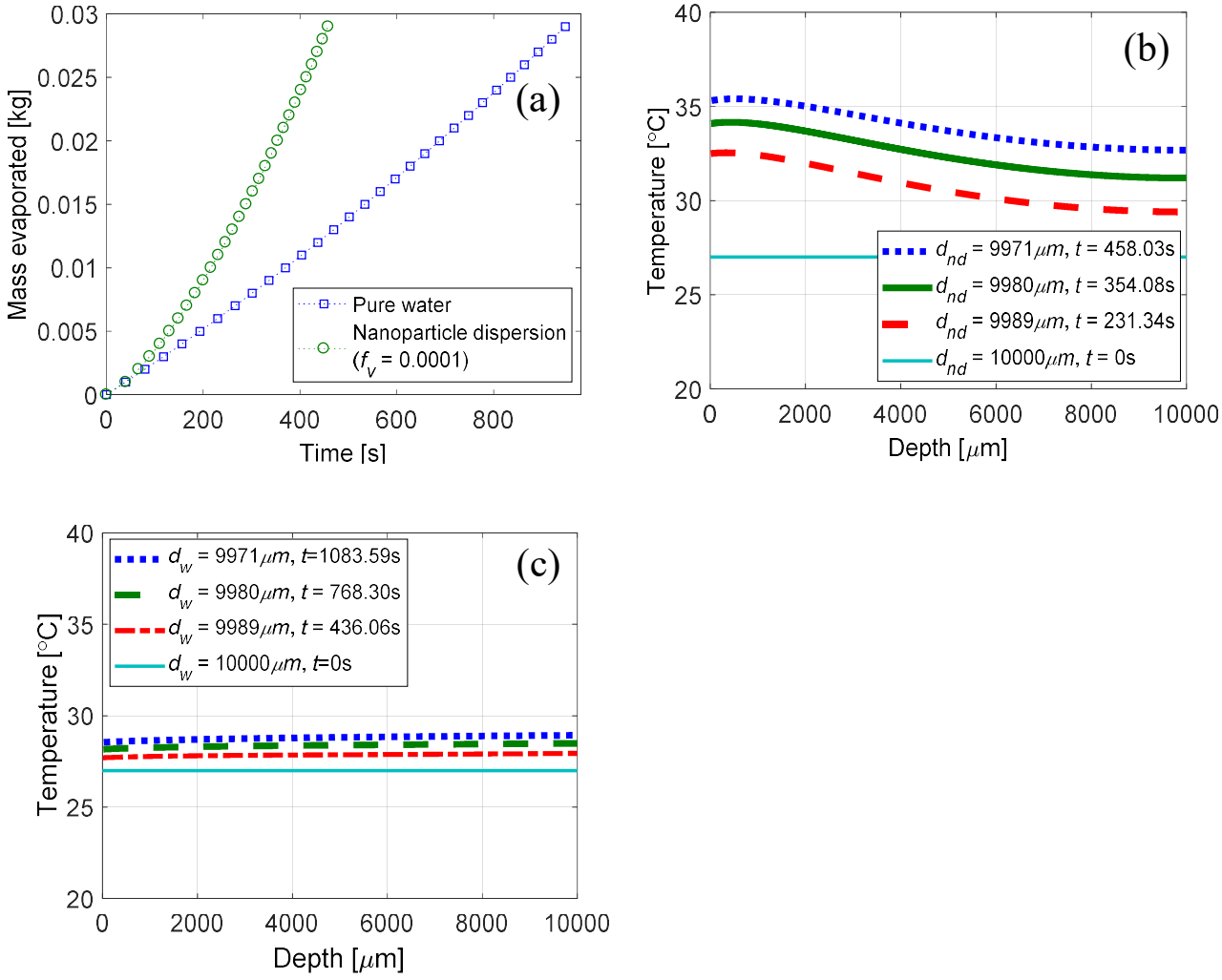

Fig. 5 (a) Mass evaporated as a function of time; temperature distribution and liquid depth evolution in case of (b) nanoparticle dispersion, and (c) pure water.

Now it is revealed that addition of nanoparticles have significant impact on the evaporation rate, the next step is to identify the key parameters that impact this evaporation rate. This has been done by varying the magnitude of the concerned parameter and keeping all the other parameters fixed. Namely, the effect of nanoparticle volume fraction, nanoparticle diameter, and ambient conditions (ambient temperature, relative humidity, wind speed, and solar irradiance) have been

studied in the present work. The subsequent sections detail the effect of varying each one of the aforementioned parameters on the evaporation rate.

5.2 EFFECT OF MAGNITUDE OF SOLAR IRRADIANCE:

Solar irradiance may vary due to cloud cover, latitude, time of the day, season etc. Furthermore, concentrated solar energy may be utilized for evaporating (and hence purifying) water. Here we have varied the magnitude of the solar irradiance, while keeping all the other parameter fixed. Figure 6 shows that there is a significant increase in evaporation rate with increase in solar irradiance. Hence addition of nanoparticles to the water coupled with concentrated solar power could result in high evaporation rates and hence high pure water yield.

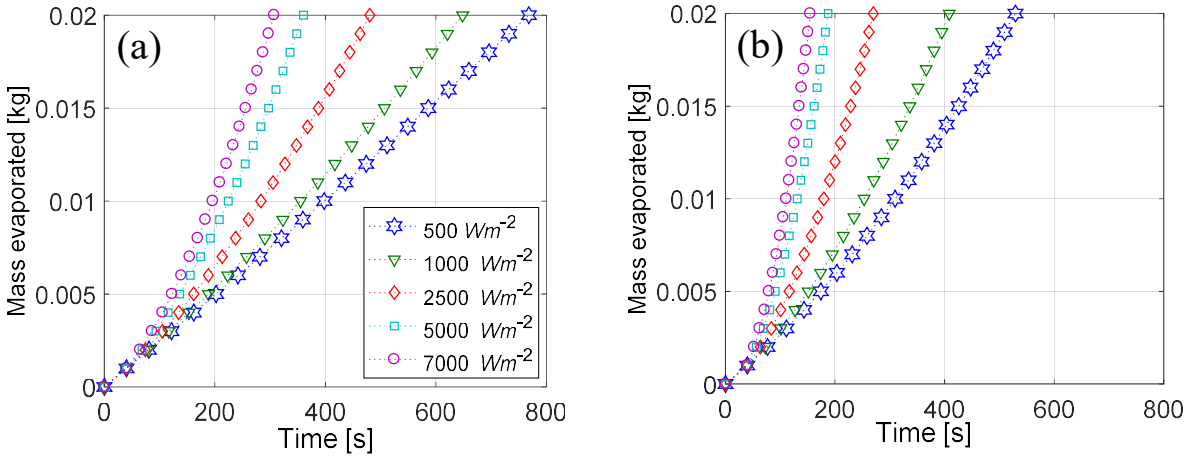

Fig. 6 Effect of magnitude of solar irradiance on the evaporation rate of (a) pure water, and (b) amorphous carbon based nanoparticle dispersion. $f_v = 0.00001$.

5.3 EFFECT OF AMBIENT TEMPERATURE AND RELATIVE HUMIDITY:

Ambient temperature and relative humidity of humid air play a significant role in dictating the evaporation rate. In order to quantify the effect of these, realistic combinations of ambient temperature and relative humidity have been chosen. This has been done by studying the evaporation rates in various regions across the globe that has some characteristic ambient conditions. Table 4 details the ambient conditions (namely ambient temperature and relative humidity) of various cities, these cities have so chosen that most of the typical ambient conditions could be studied. Furthermore, these values have been taken for the two distinct months of the year (January and June).Figure 7(a) and (b) show the evaporation rate for the aforementioned cities in the month of June and January respectively.

Table 4. Average temperature and relative humidity in five different cities of the world in the month of June and January [39-44].

City	In the month of June		In the month of January	
	Average R.H.(%)	Average (^{o}C) Temperature	Average R.H.(%)	Average Temperature (^{o}C)
Dubai	58	37	65	24
Mumbai	80	32	69	30
London	73	15	81	8.1
Aswan (Egypt)	18	25	40	10
New York	65	26	61.5	3.5

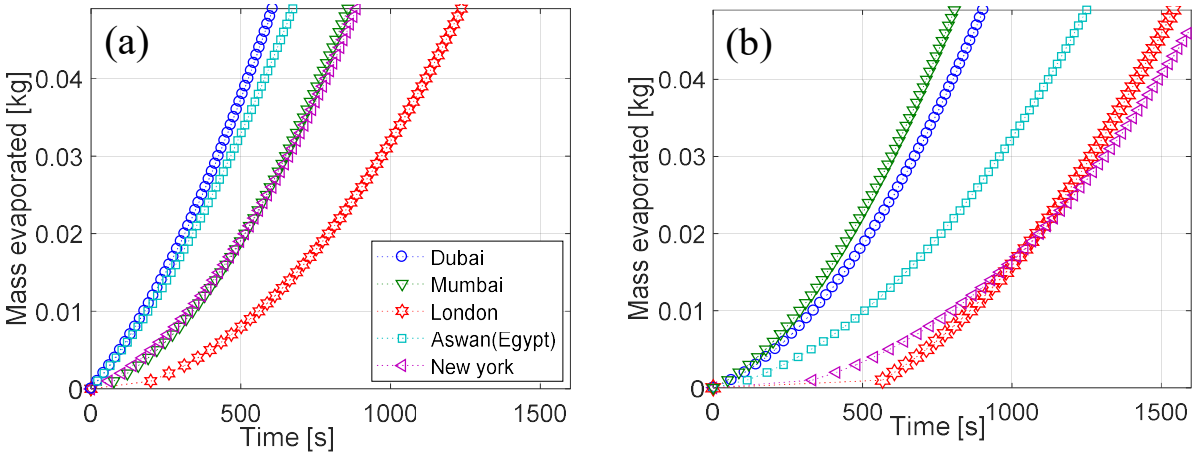

Fig. 7 Mass evaporated as a function of temperature for five different cities in the month of (a) June, and (b) January. f_v = 0.00001.

5.4 EFFECT OF WIND SPEED:

Wind speed above the liquid free surface impact the convective heat and mass transfer coefficients and hence the evaporation rate. Figure 8 shows that with increasing the wind speed the evaporation rate increases. The enhancement in evaporation rate is high at high wind velocities.

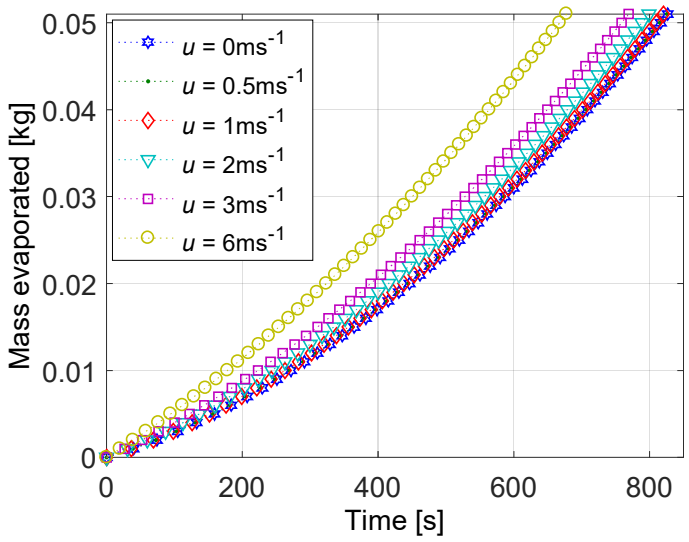

Fig. 8 Effect of wind speed on the evaporation rate. $f_v = 0.00001$.

5.5 EFFECT OF NANOPARTICLE DIAMETER:

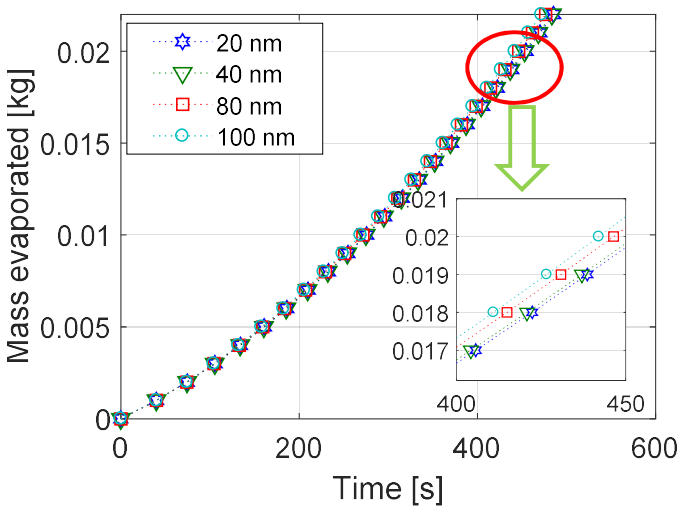

Fig. 9 Effect of nanoparticle diameter on the evaporation rate. $f_v = 0.00001$.

Next, the effect of varying nanoparticle diameter has been evaluated. It can be clearly seen from Fig. 9 that although the evaporation rate increases with increase in nanoparticle diameter, but the enhancement is negligibly small. Thus indicating that increasing the volume fraction is far more effective as compared to increasing the diameter of the nanoparticles, in order to enhance the evaporation rate.

5.6 EFFECT OF NANOPARTICLE VOLUME FRACTION:

Figure 10 details the effect of different nanoparticle volume fractions on the evaporation rate (while keeping all other parameters fixed). The curves reveal that evaporation rate increases when volume fraction of the nanoparticles increases. However, the magnitude of evaporation rate enhancement tends to decreases after a certain volume fraction. This may be ascribed to the fact that as the volume fraction of nanoparticles is increased, the solar irradiance absorption capability (and hence the evaporation rate) increases. However, after a certain value of volume fraction, nanoparticle dispersion reaches its saturation value, and any further increase in volume fraction does not significantly impact the solar irradiance absorption capability.

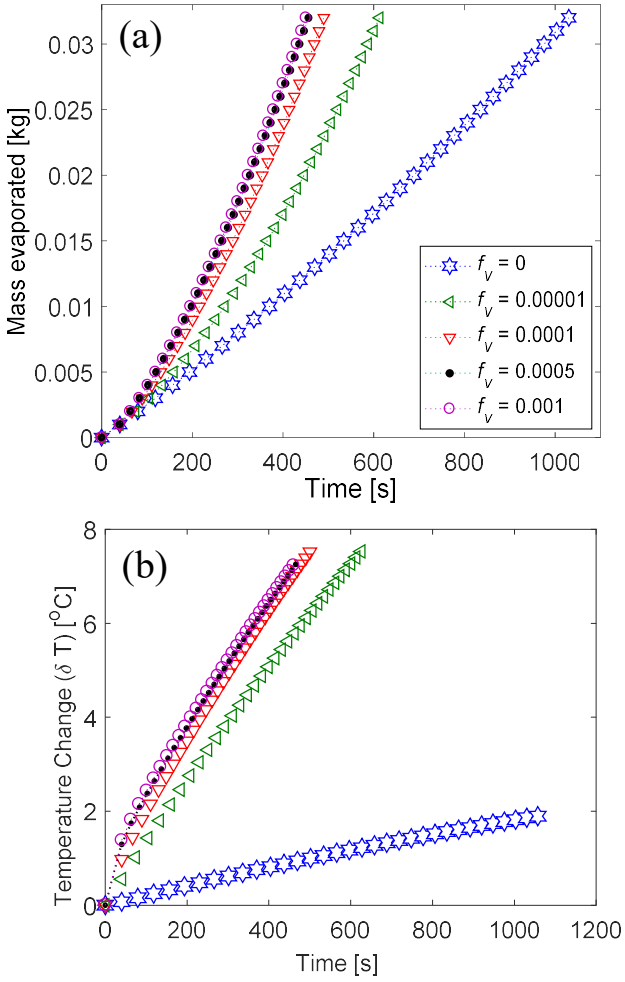

Fig. 10 Effect of nanoparticle volume fraction on the (a) evaporation rate, and (b) the temperature change of the nanoparticle dispersion.

Overall, the parametric study relevant to the evaporation rate during volumetric heating reveals that among the various parameters, nanoparticle volume fraction and the incident solar irradiance are the two parameters that have the most significant impact on the evaporation rate. Furthermore, the nanoparticle diameter has been found to have the least impact on the evaporation rate.

CHAPTER 6

EXPERIMENTAL MATERIAL AND METHODS

To continuously monitor the evaporation rate, the setups were loaded on to an analytical weighing balance (METTLER TOLEDO XSE104) which could give real time values during the evaporation process. Figure 11 shows the pictures as well as the schematics of the experimental setups, which are essentially similar in all respects except for the bottom surfaces.

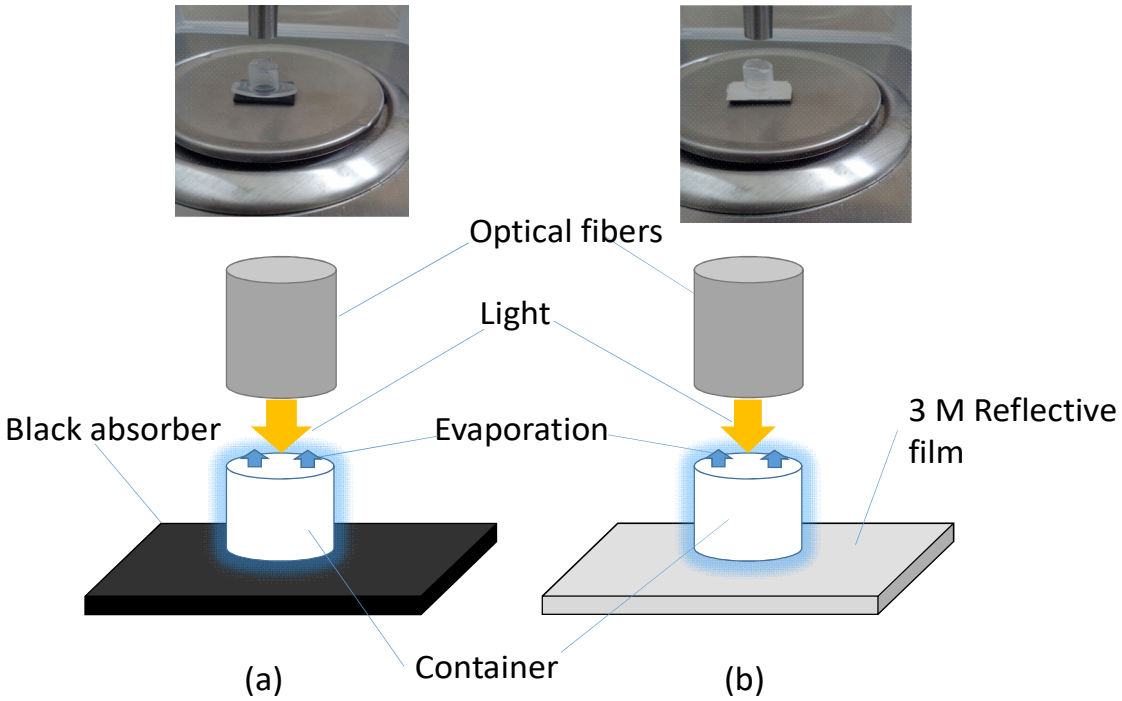

Fig. 11 Photographs and schematics of experimental setups with (a) black and (b) reflective bottom.

In our experiment we have used sewage water as the basefluid. To find out difference in evaporation rates at different mass fractions of amorphous carbon nanoparticles, all the experiments were done at similar ambient conditions (ambient temperatures and relative humidity). The prepared nanofluid was filled into the setups and heated volumetrically with help of a light source connected with optical fibers (light guides). K type thermocouples were employed to measure the temperature distribution and the ambient temperature, and a wet and dry bulb hygrometer was used (ZEAL England P501) to measure the relative humidity. Table 5 details the ambient temperatures and relative humidity values during the experimentation.

For each mass concentration at least three experiments were carried out to ensure repeatability. This was repeated for both the bottom conditions - black and reflective.

For getting a sizable amount of distillate, a separate setup has been fabricated which was then employed to produce distillate under the sun. Figure 12 shows the photograph and schematic of the same.

There is a small selectively coated (black chrome) metallic container housing the nanofluid (sewage water + amorphous carbon nanoparticles). This container is enveloped with a glass cover which allows the sunlight to interact with the nanofluid as well as serves as the surface on which condensation happens.

Total dissolved solids in sewage and distilled water were calculated experimentally in the lab by evaporating the water and then weighing the residue that left behind after evaporation. pH was measured with a pH meter (THERMO ELECTRON)

Table 5 Ambient conditions during the evaporation rate measurement experiments.

Bottom Surface	Mass Fraction, mgl^{-1}	Ambient Temperature °C (Error)	Relative Humidity, % (Error)
Black	200	26.5(±0.61)	71%(±2.44)
	100	26.5(±0.70)	71%(±6.16)
	50	26.6(±0.37)	73.3%(±0.81)
	0	26.7(±0.73)	72.3%(±4.08)
3M Reflective	200	26.8(±0.37)	73.3%(±1.63)
	100	26.5(±0.56)	77%(±4.24)
	50	26.6(±0.73)	70.3%(±8.98)
	0	26.9(±0.36)	68.9%(±5.79)

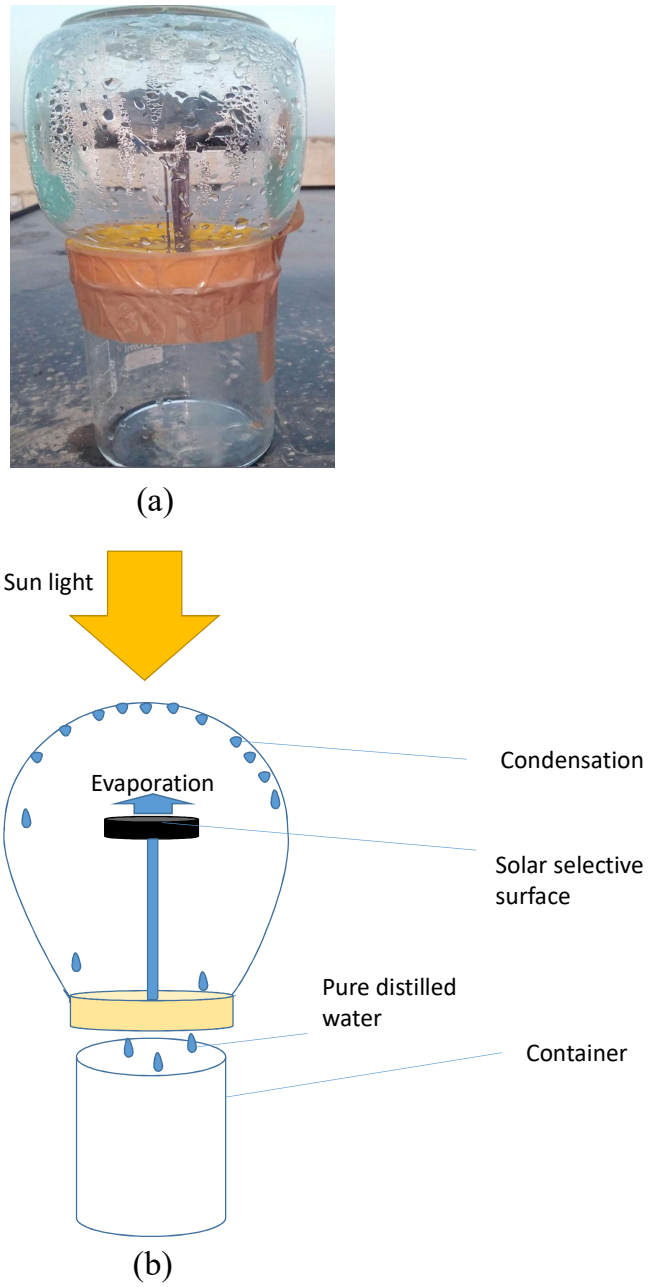

Fig. 12 Photograph and schematic of the experimental setup employed for distillate generation.

CHAPTER 7
EXPERIMENTAL RESULTS

Experimental evaluation of the evaporation rates for the two cases of bottom surfaces at various mass fractions of the nanoparticles have been plotted in Fig. 13.

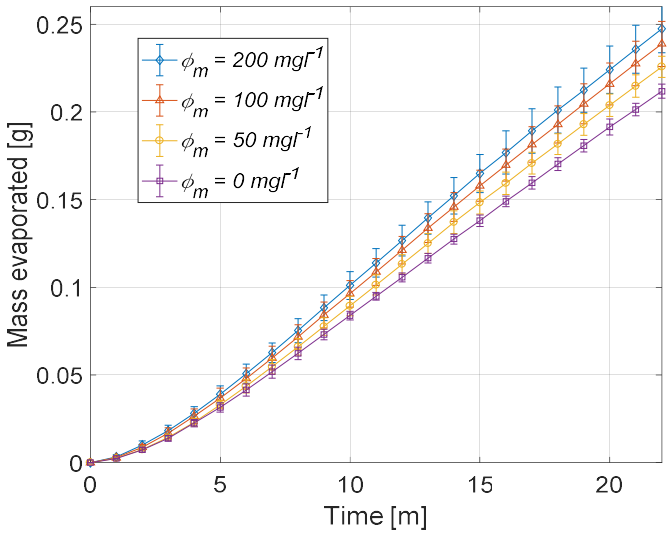

(a)

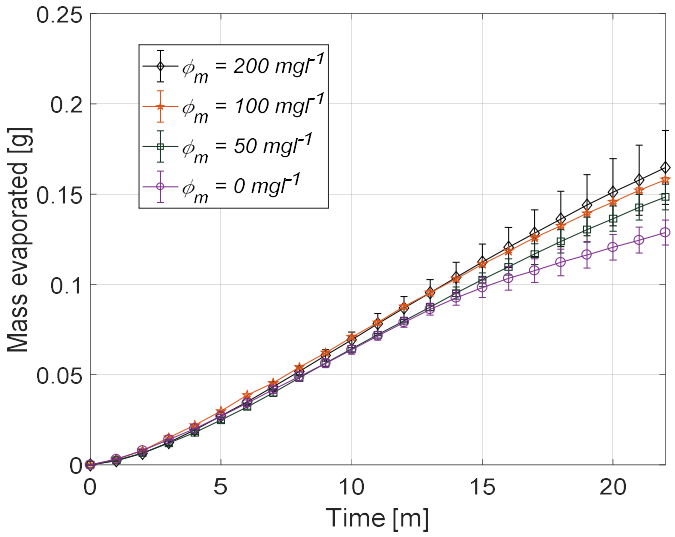

(b)

Fig. 13 Graphs showing the mass of water evaporated as a function of time for four different mass fractions of nanoparticles for (a) black bottom and (b) reflective bottom surfaces respectively.

Plots in Fig. 14 clearly reveal that for a given illumination period (22 minutes in the present study), the total mass evaporated increases when mass fraction of the nanoparticles increases. Furthermore, black bottom is far more effective than a reflective bottom clearly indicating the criticality of choosing the bottom surface.

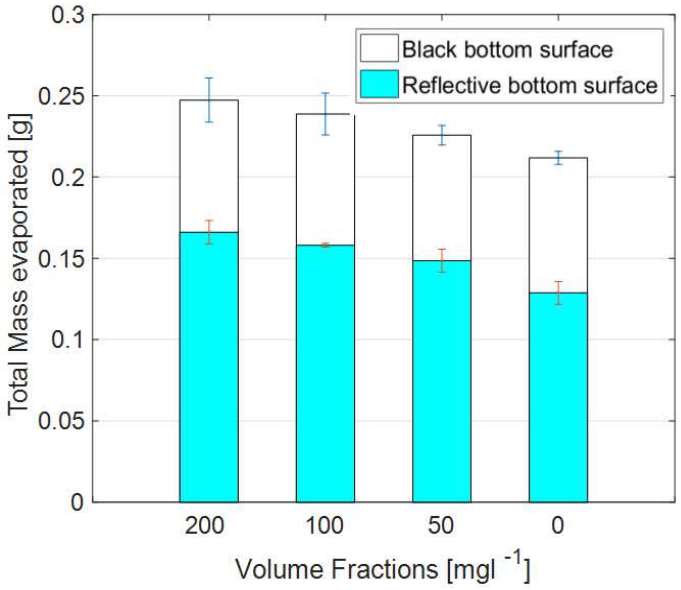

Fig. 14 Mass evaporated as a function of nanoparticle mass fraction for black and reflective bottom cases.

Furthermore, in order clearly understand the reasons for evaporation rate enhancements; temperature distribution in each case was also recorded. Figure 15 shows the temperature at top and bottom layer of nanofluid during evaporation for different mass fractions for the black and reflective bottom cases. Figure 16, shows the average temperature in four different mass fractions of nanofluid for black and reflective bottom surfaces respectively. Higher mass fractions nanofluid has higher temperature than lower mass fractions. In case of black bottom surface average temperature is higher than reflective bottom surface.
Finally, the collected distillate in outdoor experiments and the sewage water TDS and pH results (tabulated in Table 6) clearly indicate that it is indeed possible to considerably reduce the TDS and achieve favorable pH through volumetrically heating of sewage water. Figure 17 shows the photographs of the sewage water sample before and after purification.

Table 6 Properties of sewage water sample before and after distillation.

Properties	Sewage water	Distilled water
Color	Yellowish	Colorless
Odor	Stale	Odorless
Ph	9.04	7.49
TDS	743 mgL^{-1}	126.5 mgL^{-1}

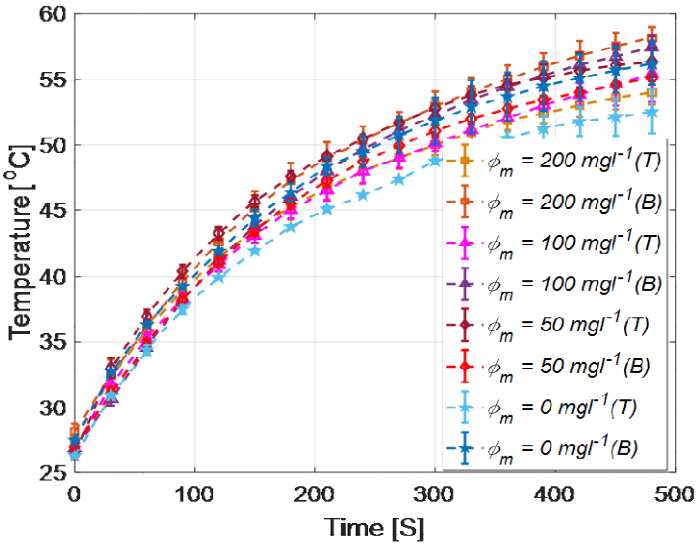

(a)

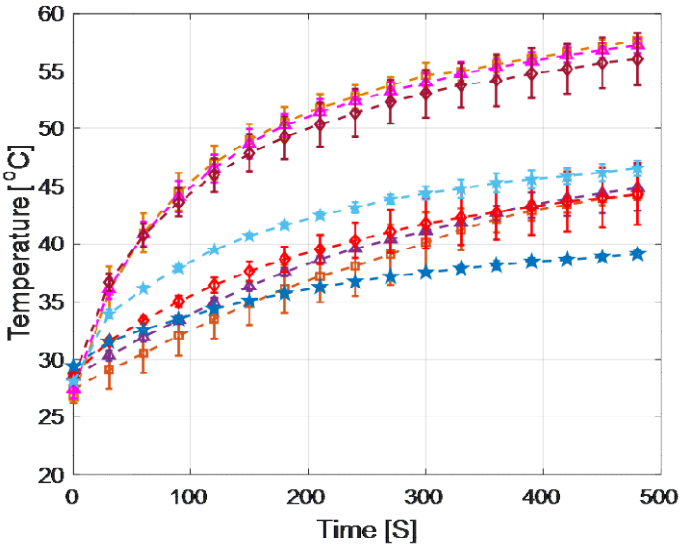

(b)

Fig.15 Graphs showing the temperature at bottom (B) and top (T) layer in nanofluid as a function of time for four different mass fractions of nanofluid having (a) black bottom surface, and (b) reflective bottom surfaces respectively.

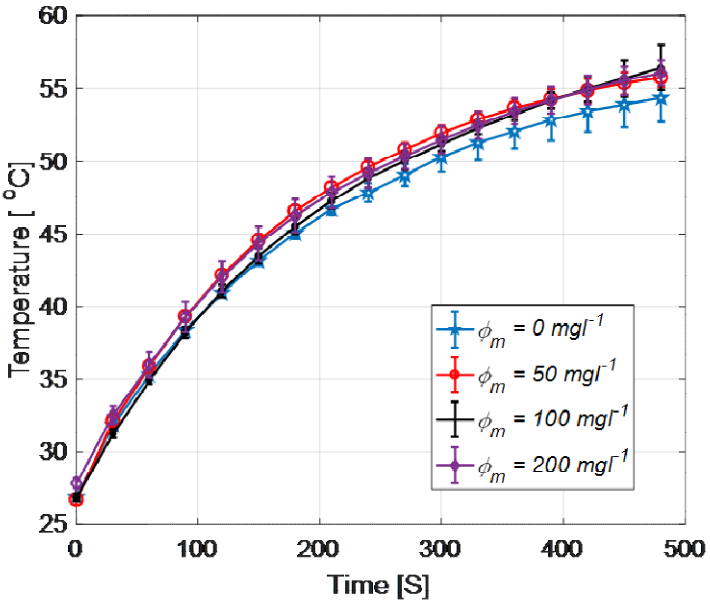

(a)

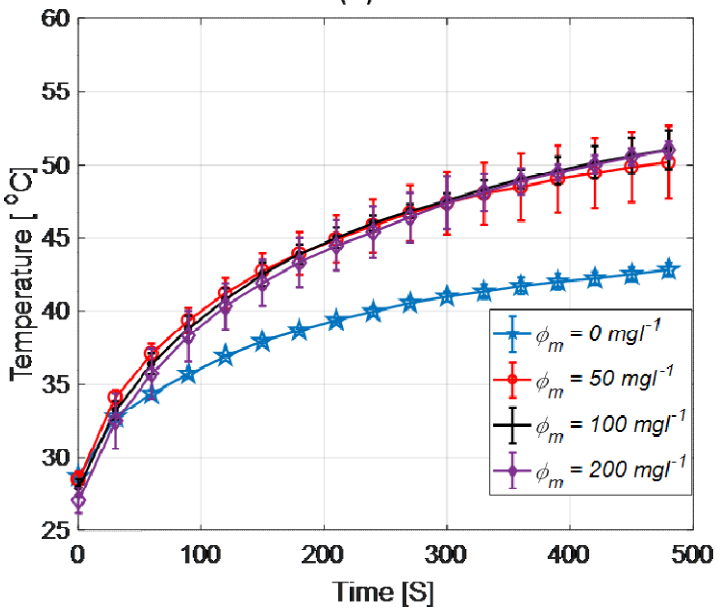

(b)

Fig.16 Graph showing the average temperature in nanofluid as a function of time for four different mass fractions of nanofluid having (a) Black bottom surface, and (b) 3M film reflective bottom surface.

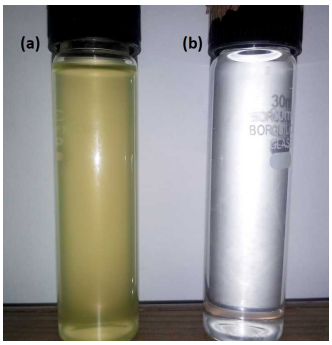

Fig. 17 Photographs of the sewage water sample (a) before and (b) after purification.

CHAPTER 8
VALIDATION OF THE DEVELOPED THEORETICAL MODEL

8.1 VALIDATION OF THE THEORETICAL MODEL WITH ISHII ET AL.

In order to validate the developed theoretical model for predicting the evaporation rate during volumetric heating, I have compared the results of the present work with that of experimental work recently reported by Ishii et al [28].
In order to aid validation, we have tried to keep all the operating parameter in our theoretical model similar to those in Ishii et al. Table 7 details these parameters and provides a comparison of the input parameters in the two works.

Table 7 Comparing parameters between the input parameter in the present theoretical work and the experimental study of Ishii et al.

		Ishii et. al., 2016	**Present study**
Type of study		Experimental	Theoretical
Nanoparticles	**Material**	Silicon	Silicon
	Size	Average particle size = 80nm	80 nm
	Shape	Spherical	Spherical
Basefluid		Water	Water
Light Source		Solar simulator	Sun, approximated as black body at 5800K
Aperture area		0.00138544 m^2	0.00138544 m^2
Flux		800Wm^{-2}	800Wm^{-2}
Ambient conditions	**Air temperature**	21°C	21°C
	Relative humidity	41 (%)	41(%)

Aforementioned parameters have been employed in the developed theoretical model to predict the mass evaporated as a function of time. Furthermore it has been compared with that of Ishii et al (see Figs. 18 and 19).

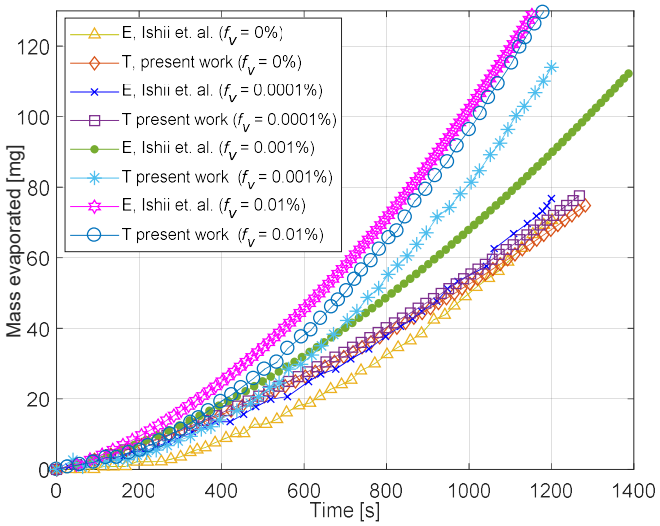

Fig. 18 Comparing the evaporated rate as predicted by the present theoretical model (PTM) with that of Ishii et al.

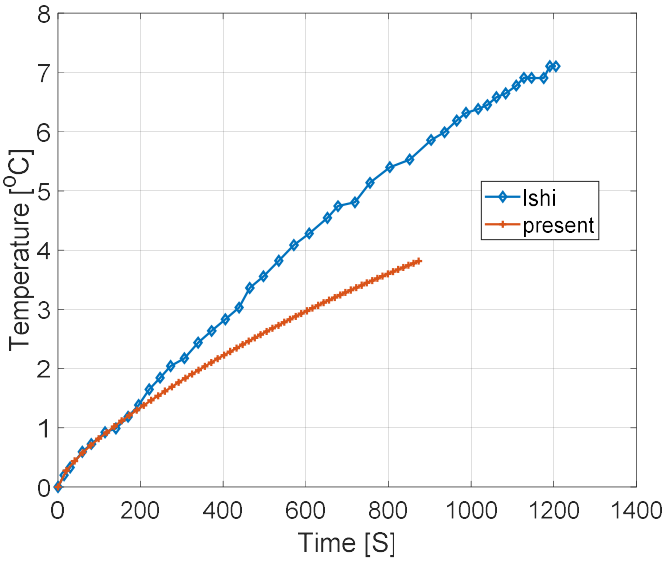

Fig. 19 Comparing the temperature as predicted by the present theoretical model (PTM) with that of Ishii et al for same amount of water evaporated in case of pure water.

Comparison of the two works reveals that the theoretical model is quite accurate in predicting the evaporation rate in case of pure water. However, in case of nanoparticle dispersions, the PTM overestimates the evaporation rate. Furthermore, the difference between the two works is more pronounced at high nanoparticle volume fractions.

The reason for mismatch at high nanoparticle fractions is expected due to the fact that at high volume fraction, the nanoparticles tend to form soft agglomeration and hence settle down or tend to occupy positions far from the free surface, due to which effective nanoparticle concentration is expected to reduce in real life experimentation (if the stability is not taken care of, as was the case with Ishii et al.). However, this type of phenomenon has not been accounted for in the

present theoretical model. Although in the experimental work of Ishii et al., the average particle size has been reported as 80nm, but it has also been reported that there was nanoparticle distribution with size varying from 40nm to 250nm. Whereas in the present theoretical model we have assumed that all the particles are having 80nm diameter. As a part of future work, the authors intend to study in detail the effect of nanoparticle agglomeration on the evaporation process.

Figure 19 shows the increase in temperature during evaporation for present theoretical modal and experimental work of ishii et al. This temperature increase is for same amount of water evaporated (80 mg).

On the whole, the theoretical model developed in the present work can accurately predict the evaporation rate of nanoparticle dispersions during volumetric heating. Furthermore, the model is robust enough to predict the impact of host of parameters on the evaporation rate of nanoparticle dispersions in particular and participating media in general.

8.2 VALIDATION OF THE THEORETICAL MODEL WITH PRESENT EXPERIMENTAL WORK:

We have also validated the theoretical work with experimental work that we have already discussed above. In experiments we have used four volume fractions of amorphous carbon nanofluids. We have compared the evaporation rates and temperature distributions of experiments with theoretical model developed by writing a code in MATLAB. Figure 20 compares the evaporation rates of experiments and theoretical model for pure water. Figure 21 shows the temperature at top and bottom layers of water for theoretical and experimental work when bottom surface is reflective. Both are not perfectly matched because of different conditions. Experimentally bottom and side walls are not perfectly insulated, thus heat can loose from these sides. Graph shows that bottom and top layer temperature in case of experiments increases parabolic ally. On the other hand in case of theoretical results bottom layer temperature increases linearly. The reason is that in theoretical model we have considered side and bottom surfaces as insulated. Thus there is no heat loss from the bottom and side walls in case of theoretical work.

Table 8 Comparing parameters between the input parameter in the present theoretical work and the present experimental study.

		Present study	**Present study**
Type of study		Experimental	Theoretical
Nanoparticles	**Material**	Amorphous carbon	Amorphous carbon
	Size	Average particle size = 80nm	80 nm
	Shape	Spherical	Spherical
Basefluid		Water	Water

Light Source		Optical fiber	Sun, approximated as black body at 5800K
Aperture area		63.61 mm^2	63.61 mm^2
Flux		18500Wm^{-2}	18500Wm^{-2}
Ambient conditions	**Air temperature**	26.9°C	26.9°C
	Relative humidity	68.9 (%)	68.9(%)

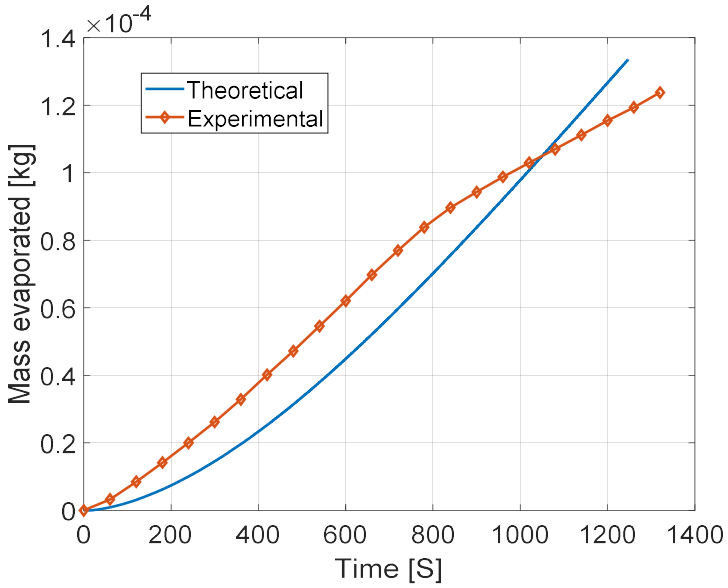

Fig. 20 Comparing the evaporated rate as predicted by the present theoretical model (PTM) with that of present experimental work.

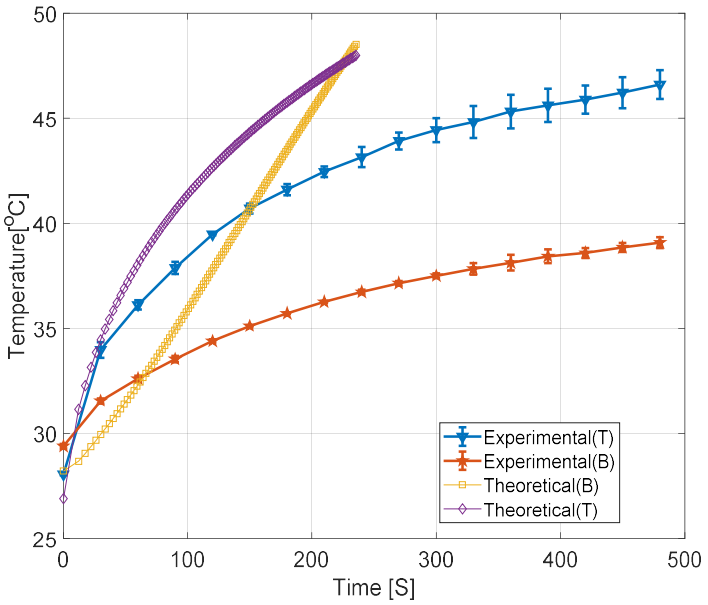

Fig. 21 Comparing the temperature distribution at top (T) and bottom (B) layers as predicted by the present theoretical model (PTM) with that of present experimental work.

CHAPTER 9
CONCLUSIONS AND FUTURE WORK

A comprehensive theoretical model has been developed to predict the evaporation rate when solar irradiance directly interacts with the nanoparticle dispersion. Theoretical results indicate that addition of trace amounts (f_v = 0.0001) of amorphous carbon nanoparticles can significantly increase the evaporation rate (~58% higher than in the case of pure water). Among the various parameters, nanoparticle volume fraction and solar irradiance have been found to significantly impact the evaporation rate. It has been found that the volume fraction of nanoparticles can be increased only up to a certain limit, after which the effect of increasing volume fraction does not enhance the evaporation rate further. Furthermore, the effect of size of nanoparticles has negligible effect in enhancing evaporation rate.

Experimental results indicate that addition of amorphous carbon particles can effectively improves the vaporization of water. Experimental work concludes that to enhance the evaporation of water during various heating applications and distillation process nanoparticles can be used. The present work clearly reveals that if we use solar selective coating at bottom surface in addition of nanoparticles in water efficiency of solar still increases effectively. On the other hand results indicates a large difference in color, odor, PH and TDS between sewage and distilled water. This shows that solar distillation process is a reliable source to get fresh water.

When we compare the theoretical and experimental results it shows that evaporation rates are higher in theoretical results of nanofluid as compared to the experimental results. This may be attributed to the fact that nanoparticles are not homogeneously dispersed in base fluid. it is suggested that to increase the stability of nanofluids, nanoparticles need to be functionalized.

REFERENCES

[1] Andreozzi, R., Caprio, V., Insola, A., Marotta, R., "Advanced oxidation processes (AOP) for water purification and recovery." Catalysis Today, Vol. 53, pp.51-59 (1999)

[2] Carlos A. Huitle, M.and Ferro, S.,"Electrochemical oxidation of organic pollutants for the wastewater treatment: direct and indirect processes." Chemical society Reviews., Vol. 35, pp. 1324-1340(2006)

[3] Das, R., Md. E., Ali., Hamid, S., B., A., Ramakrishna, S., Chowdhury, Z., Z., "Carbon nanotube membranes for water purification: A bright future in water desalination." Desalination, Vol. 336, pp. 97-109, (2014)

[4] Malik, M., A., Ghaffar, A. and Malik, S., A.,"Water purification by electrical discharges." Plasma Sources Sci. Technol., Vol. 10, pp. 82–91 (2001)

[5] Shannon, M., A., Bohn P., W., Elimelech M, Georgiadis J., G., Marin B., J., &Mayes A., M., "Science and technology for water purification in the coming decades." Nature Publishing Group, Vol. 452, pp. 301-310, (2008)

[6] McCarty, P., L., Bae J., and Kim, J., "Domestic Wastewater Treatment as a Net Energy Producer." Vol. Environmental Science & Technology., Vol. 45, pp. 7100-7106 (2011)

[7] Vinoth, K. K., Kasturi, B.R., "Performance study on solar still with enhanced condensation." Desalination, Vol. 230, pp.51–61 (2008).

[8] Al-Hayek, I., Badran, O. O., "The effect of using different designs of solar stills on water distillation." Desalination, Vol.169, pp. 121-127 (2004).

[9] Sharaf, M. A., "Thermo-Economic comparisons of different types of solar desalination processes." Journal of Solar Energy Engineering, Vol. 138 (2), pp. 1-10 (2015).

[10] Lavan, Z., Assouad, Y., "Solar desalination with latent heat recovery." Journal of Solar Energy Engineering, Vol. 110(1), pp. 14-1 (2009).

[11] Aburideh , H. , Deliou , A., Abbad , B., Alaoui , F., Tassalit , D. and Tigrine, Z. , "An Experimental Study of a Solar Still: Application on the sea water desalination of Fouka." Vol. 33, pp. 475-484 (2012)

[12] Hanson, A., Zachritz, W., Stevens, K., Mimbela, L., Polka, R., Cisneros, L.,"Distillate water quality of a single- basin solar still: laboratory and field work." ,Solar Energy, Vol. 76, pp. 635-645 (2004)

[13] Sharon, H., Reddy, K., S., Krithika,D., Philip,L., "Experimental performance investigation of tilted solar still with basin and wick for distillate quality and enviro-economic aspects." Desalination, Vol. 410, pp. 30-54 (2017)

[14] Joe Patrick Gnanaraj, S., Ramachandran, S., Santosh Christopher, D., "Enhancing the design to optimize the performance of double basin solar still." Desalination, Vol. 411, pp. 112-123 (2017)

[15] Panchal, H., N., “Enhancement of distillate output of double basin solar still with vacuum tubes.” ,Journal of King Saud University – Engineering Sciences., Vol. 27, pp. 170-175 (2015)

[16] Ayber, H., S., “A review and comparison of solar distillation: Direct and indirect type systems.”Desalination and Water Treatment., Vol. 10, pp. 321-331 (2009)

[17] Sathyamurthy, R., Samuel, D., G., H., Nagarajan, P.,K., & Arunkumar T., “Geometrical variations in solar stills for improving the fresh water yield.”, Desalination and Water Treatment., Vol.10, pp.1-15 (2016)

[18] Panchal, H., N., & Shah, P.,K.,“Investigation on performance analysis of a novel design of the vacuum tube-assisted double basin solar still: an experimental approach.” International Journal of Ambient Energy. (2014)

[19] Balan, R. ,Chandrasekaran, J., Shanmugan, S., Janarthanan, B.& Kumar, S.”Review on passive solar distillation.” Vol. 28, pp. 217-238 (2012)

[20] Panchal, H., Patel, N., & Thakkar, H., “Various techiques for improvement in distillate output from Active solar still.”International Journal of Ambient Energy. pp 1-37 (2015)

[21] Qasim, S., R., “Treatment of domestic sewage by using solar distillation and plant culture.” Journal of Environmental Science and Health., Vol. 13, pp. 615-627, (2008)

[22] Tyagi, H., Phelan, P., Prasher, R., "Predicted efficiency of a low-temperature nanofluid-based direct absorption solar collector." Journal of Solar Energy Engineering, 131(4), pp. 041004 (2009).

[23] Lenert, A., Wang, E. N., "Optimization of nanofluid volumetric receivers for solar thermal energy conversion." Solar Energy, 86(1), pp. 253–265 (2012).

[24] Lee, B., J., Park, K., Walsh, T., Xu, L., “Radiative heat transfer analysis in plasmonic nanofluids for direct solar thermal absorption.” Journal of Solar Energy Engineering, Vol. 134(2), pp.1-6 (2012).

[25] Khullar, V., Tyagi, H., Hordy, N., Otanicar, T., Hewakuruppu, Y., Modi, P., Taylor, R.., “Harvesting solar thermal energy through nanofluid-based volumetricabsorption systems.”International Journal of Heat and Mass Transfer, Vol.77, pp.377–384 (2014).

[26] Khullar, V., Tyagi, H., Bhalla, V., “Potential heat transfer fluids (nanofluids) for direct volumetric absorption-based solar thermal systems.” Journal of Thermal Science and Engineering Applications, Vol. 10(1), pp.01100984 (2017).

[27] Gan, Y., Qiao, L., “Optical properties and radiation enhanced evaporation of nanofluid fuels containing carbon-based nanostructures.”Energy fuels 2012, Vol . 26, pp. 4224 4230. (2012).

[28] Ishii, S., Sugavaneshwar, R. P., Chen, K., Dao, T., D., Nagao, T., “Solar water heating and vaporization with silicon nanoparticles at Mie resonances.” Optical Materials Express, Vol. 6, pp.640-648 (2016).

[29] Brewster, M., Q.. Thermal radiative transfer and properties. John Wiley and Sons. (1992).

[30] Stagg, B. , J. , Charalampopoulos,T. T.,"Refractive indices of pyrolytic graphite, amorphous carbon, and flame soot in the temperature range." Combustion and Flame, Vol., 94, pp.381-396(1993).

[31] Moran, N., "Optical properties of fine amorphous carbon grain in infrared region." Astrophysics and Space Science, Vol.172, pp.21-28(1990).

[32] Bohren, C.,F., Huffman, D. R., Absorption and scattering of light by small particles. A Wiley-Interscience John Wiley and Sons (1983).

[33] Incropera, F. P., Dewitt, D. P., Fundamentals of heat and mass Transfer, fifth ed., John Wiley and Sons, New York, pp. 465–531 (2002).

[34] Cengel, Y., A., Ghajar, A., Heat and Mass Transfer Fundamental and Applications , fifth ed., McGraw-Hill Education, 2 Penn Plaza, New York, pp. 424-472,534-596,835-906.

[35] Fundamentals of Heat Transfer by Incropera and DeWitt, Wiley, 5th Edition, (2002)

[36] Iskra, C., R., Simonson, C., J., " Convective Mass Transfer between a hydrodynamically developed airflow in a short rectangular duct." International Journal of Heat and Mass Transfer., Vol. 50, pp. 2376-2393 (2007)

[37] Boukadida, N., Nasrallah, B., S., " Mass and heat transfer during water evaporation in laminar flow inside a rectangular channel- validity of heat and mass transfer analogy." Int. J. Therm. Sci.,Vol. 40, pp.67–81 (2001).

[38] Zabalegui, A., "Investigation of thermal properties and heat reduction mechanisms in nanofluid phase change materials." (Degree of Master of Science In Mechanical Engineering In the School of Engineering at Santa Clara University, June 2013 Santa Clara, California 2013).

[39] Ambient temperature and relative humidity of Dubai https://web.archive.org/web/20131004223556/https://services.dubaiairports.ae/dubaimet/MET/Climate.aspx (accessed on 8th December 2017)

[40] Ambient temperature and relative humidity of Mumbai https://www.weather2travel.com/climate-guides/india/mumbai.php (accessed on 8th December 2017)

[41] Ambient temperature and relative humidity of London http://www.weatheronline.co.uk/weather/maps/city?LANG=en&PLZ=_____&PLZN=_____&WMO=03779&CONT=ukuk&R=0&LEVEL=162&REGION=0003&LAND=UK&MOD=tab&ART=TMX&NOREGION=1&FMM=1&FYY=2001&LMM=12&LYY=2014 (accessed on 8th December 2017)

[42] Ambient temperature and relative humidity of Aswan (Egypt) http://worldweather.wmo.int/en/city.html?cityId=1272 (accessed on 8th December 2017)

[43] Ambient temperature and relative humidity of New york city https://www.currentresults.com/Weather/New-York/humidity-july.php (accessed on 8th December 2017)

[44] Ambient temperature and relative humidity of Dubai: http://www.dubai.climatemps.com/humidity.php (accessed on 8th December 2017).

LIST OF PUBLICATIONS FROM THE PRESENT WORK

- Using Solar Energy for Water Purification Through Nanoparticles Assisted Evaporation, revision under review at ASME Journal of Solar Energy Engineering - Including Wind Energy and Building Energy Conservation (Accepted for publication).
- Experimental Investigation into the Applicability of Nanoparticles in Purification of Sewage Water Through Usage of Solar Energy, (submitted as book chapter for the monograph entitled “Advances in Solar Energy”, under review)

Thesis VIRENDER

ORIGINALITY REPORT

13%	8%	10%	%
SIMILARITY INDEX	INTERNET SOURCES	PUBLICATIONS	STUDENT PAPERS

PRIMARY SOURCES

1	ethesis.nitrkl.ac.in Internet Source	1%
2	www.coursehero.com Internet Source	1%
3	Vikrant Khullar, Himanshu Tyagi, Todd P. Otanicar, Yasitha L. Hewakuruppu, Robert A. Taylor. "Solar Selective Volumetric Receivers for Harnessing Solar Thermal Energy", Journal of Heat Transfer, 2018 Publication	1%
4	docslide.us Internet Source	<1%
5	Vishal Bhalla, Himanshu Tyagi. "Parameters influencing the performance of nanoparticles-laden fluid-based solar thermal collectors: A review on optical properties", Renewable and Sustainable Energy Reviews, 2018 Publication	<1%
6	Khullar, Vikrant, Himanshu Tyagi, Patrick E. Phelan, Todd P. Otanicar, Harjit Singh, and	<1%